

*Peculiarities of formation of microstructure in composites based on chemically synthesized zirconium nanopowders obtained by the method of decomposition from fluoride salts were considered. Hydrofluoric acid, concentrated nitric acid, aqueous ammonia solution, metallic zirconium, and polyvinyl alcohol were used. It was established that the reduction of porosity in nanopowders in the sintering process is the main problem in the formation of high-density materials.*

*Analysis of various initial nanopowders, their morphology, and features of sintering by the method of hot pressing with direct transmission of electric current was made. Peculiarities of obtaining the composites based on them with the addition of  $Al_2O_3$  nanopowders applying the electric sintering method were considered. It was shown that the increase in the content of alumina nano additives leads to an increase in strength and crack resistance of the samples due to simultaneous inhibition of abnormal grain growth and formation of a finer structure with a high content of tetragonal phase.*

*The influence of sintering modes on the formation of the microstructure of zirconium nanopowders has been studied for different contents of alumina additives. Electric current promotes the surface activity of nanopowders and its variable value promotes partial fragmentation of agglomerated grains thus affecting the composite structure.*

*Physical-mechanical properties of the obtained samples, optimal compositions of mixtures, and possibilities of improving some parameters were determined. It was found that nanopowders of zirconium dioxide obtained by the method of decomposition from fluoride salts are quite suitable for the production of composite materials with high physical and mechanical properties. They can compete with imported analogs and enable obtaining of crack resistance of  $7.8 \text{ MPa}\cdot\text{m}^{1/2}$  and strength of 820 MPa*

*Keywords: zirconium dioxide, composite materials, consolidation, microstructure, alumina, sintering, crack resistance*

UDC 620.18

DOI: 10.15587/1729-4061.2021.242503

# REVEALING SPECIFIC FEATURES OF STRUCTURE FORMATION IN COMPOSITES BASED ON NANOPOWDERS OF SYNTHESIZED ZIRCONIUM DIOXIDE

Edwin Gevorkyan

Doctor of Technical Sciences, Professor\*

Volodymyr Nerubatskyi

Corresponding author

PhD, Associate Professor

Department of Electrical Power Engineering,  
Electrical Engineering and Electromechanics\*\*

E-mail: NVP9@i.ua

Volodymyr Chyshkala

PhD, Associate Professor

Department of Reactor Construction Materials  
and Physical Technologies

V. N. Karazin Kharkiv National University

Svobody sq., 4, Kharkiv, Ukraine, 61022

Oksana Morozova

Postgraduate Student\*

\*Department of Wagon Engineering and Product Quality\*\*

\*\*Ukrainian State University of Railway Transport

Feierbakha sq., 7, Kharkiv, Ukraine, 61050

Received date 08.09.2021

Accepted date 22.10.2021

Published date 29.10.2021

**How to Cite:** Gevorkyan, E., Nerubatskyi, V., Chyshkala, V., Morozova, O. (2021). Revealing specific features of structure formation in composites based on nanopowders of synthesized zirconium dioxide. *Eastern-European Journal of Enterprise Technologies*, 5 (12 (113)), 6–19. doi: <https://doi.org/10.15587/1729-4061.2021.242503>

## 1. Introduction

The study of composites based on zirconium dioxide, especially partially stabilized ones, is relevant for a number of reasons. It is promising as a tool or structural material, for example, in designing hydro abrasive nozzles with improved mechanical properties [1] and is of great functional importance. In particular, it is used in medicine as a material for endoprostheses [2, 3] and dentures [4, 5]. This explains numerous publications on methods of obtaining and processing these composites [6, 7]. Another important factor is that zirconium compounds are widespread in the lithosphere. According to various data, Clark of zirconium is from 170 to 250 g/t. Therefore, expansion of technological capabilities for the use of this material, obtaining products with a competitive market price will contribute to the promotion of

zirconium products on the world market. Materials based on nanopowders of partially stabilized zirconium dioxide with various additives of refractory compounds are especially promising [8, 9]. It should be noted that some countries where the greatest deposits of zirconium are concentrated have no own mass production of powder of this type so far. Therefore, the study of new methods of obtaining nanopowders and products based on this material will promote the creation of preconditions for the large-scale production of zirconium dioxide nanopowders.

## 2. Literature review and problem statement

Much attention is paid to the problems of obtaining composite materials based on zirconium dioxide and deter-

mining the patterns of influence of additives, in particular alumina, on the structure of composite materials.

Nanocrystalline powders of a solid solution based on  $ZrO_2$  were obtained in [10] by means of hydrothermal synthesis in an alkaline medium and the change of their properties during heat treatment in the temperature range of 400–1,300 °C was studied. It was established that hydrothermal synthesis results in the formation of a thermodynamical nonequilibrium system including a mixture of low-temperature cubic metastable solid solution and tetragonal solid solution based on  $ZrO_2$ . However, no study on crack resistance and strength of the obtained nanocrystalline powder was performed.

Nanosized zirconium dioxide, cobalt oxide, and the phases based on them were synthesized in supercritical carbon dioxide [11]. Stabilization of cubic modification was observed at a temperature of 700 °C in samples of zirconium dioxide with an admixture of cobalt oxide. This is due to the entry of cobalt admixture into the cubic structure of zirconium oxide which prevents transition to tetragonal and monoclinic modifications. The limitation of the study consists in that regularities of the effect of additives on physical-mechanical and operational properties of the obtained composite materials based on zirconium dioxide were considered insufficiently.

Effect of surface processing of various types including pneumatic abrasion of particles on strength of various translucent materials stabilized with yttrium zirconium was measured and characterized in [12]. The type of zirconium material and surface treatment affected the strength of translucent zirconium materials. Pneumatic abrasion of particles using alumina had a slight hardening effect on 4 mol. % zirconium but had a softening effect on 5 mol. % materials. Disadvantage consists in that abrasion of particles by an air-droplet method using alumina creates roughest surfaces on all materials. Materials will have lower strength in clinically used products when machining or abrasion working by air particles since deep surfaces cannot be ground for clinical use.

Characteristics of ceramic composites consisting of various compositions of alumina and zirconium dioxide are described in [13]. A study of material characteristics was performed in terms of compaction, hardness, and crack resistance. Surface morphology and elemental composition of composite materials were studied using SEM and EDX, respectively. The disadvantage of this study consists in that sintering was carried out at a temperature of 1,150 °C which was insufficient to eliminate pores although it contributed to ceramics compaction. This requires a higher sintering temperature from 1,500 to 1,700 °C or pore infiltration with PDC resin.

Fracture toughness, flexural strength, Young's modulus, hardness, and subcritical crack growth were determined in [14] for six different alumina/zirconium composites. Flexural strength was modeled using the Weibull distribution. Fracture toughness, flexural strength, and resistance to the growth of subcritical cracks increase depending on  $ZrO_2$  content (stabilized 3 mol. %  $Y_2O_3$ ). However, the issue of dependence of microstructure in samples prepared from zirconium dioxide with the addition of alumina on tetragonal-monoclinic transitions remains unresolved.

Polycrystalline 3 mol. % material of tetragonal zirconium doped with yttrium (3 mol. %  $Y_2O_3-ZrO_2$ ) was prepared in [15] using an optimized sintering process without applying pressure. Phase change and  $Y_2O_3-ZrO_2$  particle size distribution during sintering were studied. Effect of sintering temperature on properties of  $Y_2O_3-ZrO_2$  was analyzed. Sintering temperatures of 800–1,200 °C were used

in the study. The zirconium material sintered at 1,000 °C had the smallest porosity and the best density. However, the method of preparation of the material used in the study has a risk of environmental pollution and high cost.

Production of nanoparticles based on zirconium dioxide from fluoride solutions and consolidation of  $ZrO_2-Y_2O_3$  nanopowders were investigated in [16, 17]. However, the issue of the influence of hot pressing on mechanical properties of nanopowders was not considered in [16] and the influence of material particle morphology on characteristics of the obtained materials was not studied in [17].

Application of composite material  $Al_2O_3-SiC$  as a tool material was substantiated in [18]. The microstructure of composites was considered in different modes of electric sintering. However, the issue of determining the optimal composition of initial mixtures and sintering conditions when using alumina nano additives in order to obtain improved physical and mechanical properties of material remained unresolved.

Economical thermal cycle for the production of ceramic products from submicron powders of alumina, titanium oxide, and manganese oxide was proposed in [19]. Optimal composition of material for a ceramic product with the highest physical and mechanical properties was established and optimal method of preparation of the initial charge and the sintering mode were selected. The limitation of the study consists in that thermogravimetric studies have not been performed completely for sintering with various additives. In addition, not all samples were tested for the mechanical strength of the obtained ceramic products.

Analysis of the above studies has shown that zirconium dioxide partially stabilized with yttrium oxide with the addition of alumina is a promising material for use in tribosystems with improved antifriction and anti-wear properties. When studying the properties of composites under consideration, the main attention is paid to mechanical characteristics of the material, especially crack resistance and hardness compared with the tribological properties. Also, when conducting friction and wear tests, the influence of the structure of the composites based on zirconium dioxide on wear resistance was not taken into account. Most studies did not correlate thermomechanical or tribological properties. There are almost no studies on the mutual influence and compatibility of materials of the tribosystem "ceramic composite-metal" on the friction processes in the contact zone.

Thus, the issue of identifying patterns of structure formation in the composites based on synthesized nanopowders of zirconium dioxide and the effect of alumina additives on the composite material structure needs to be addressed. In addition, reducing the cost of nanopowders, improving their quality, the use of modern methods of forming and sintering nanopowders (SPS, FAST, electric sintering) creates new opportunities for the production of composite materials with high physical and mechanical properties.

---

### 3. The aim and objectives of the study

---

The study objective consisted in identifying patterns of formation of structure in composites based on synthesized nanopowders of zirconium dioxide which will make it possible to obtain composite materials with high physical, mechanical and operational properties.

To achieve this objective, the following tasks were set:

– study the microstructure of composite materials based on chemically synthesized nanopowders of zirconium dioxide obtained by the method of electric sintering (electroconsolidation);

– identify patterns of influence of additives, in particular  $\text{Al}_2\text{O}_3$ , on the structure and physical and mechanical properties of composite materials based on synthesized specific nanopowder of zirconium dioxide, determine phase composition of the obtained nanocomposites and its features;

– determine the optimal composition of initial mixtures and sintering modes when using nano additives of alumina in order to obtain improved physical and mechanical properties of the material;

– forecast possible ways to the improvement of properties of composite materials based on zirconium dioxide with a fine microstructure.

#### 4. Materials and methods used in the study

The study used  $\text{ZrO}_2$  nanopowders partially stabilized with 3 wt. %  $\text{Y}_2\text{O}_3$  produced by Kharkiv Institute of Monocrystals (Ukraine) by precipitation of  $\text{ZrO}_2$ –3 wt. %  $\text{Y}_2\text{O}_3$  from fluoride solutions (Fig. 1).  $\text{Al}_2\text{O}_3$  nanopowders manufactured by NANOE (France) were also used (Fig. 2).

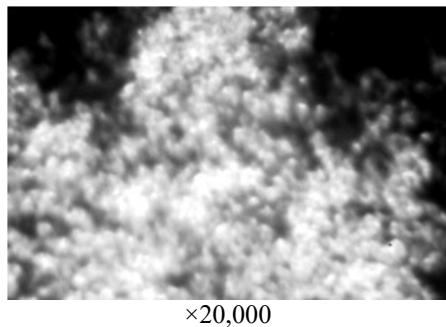


Fig. 1. General view of  $\text{ZrO}_2$ –3 wt. %  $\text{Y}_2\text{O}_3$  nanopowders obtained by precipitation from fluoride salts

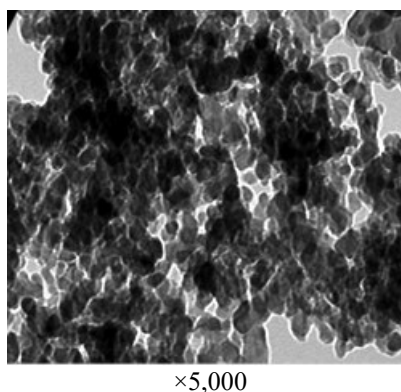


Fig. 2. General view of  $\alpha$ - $\text{Al}_2\text{O}_3$  nanoparticles manufactured by NANOE

Samples were polished in steps up to  $1\ \mu\text{m}$  on Struers grinding and polishing unit (Denmark) using diamond pastes.

The structure of electroconsolidated samples of zirconium ceramics was studied by methods of power probe microscopy (Ntegra Aura atomic-force microscope) and scanning

microscopy (Nova NanoSEM scanning ion-electron microscope, Quanta 200 3D scanning electron microscope).

AFM scanning was performed by the semi-contact method in the air in two modes: at a constant amplitude (topography) and in the mode of phase contrast. Shots of  $1\times 1\ \mu\text{m}$ ,  $2.5\times 2.5\ \mu\text{m}$  and  $5\times 5\ \mu\text{m}$  were taken.

Chemical analysis of consolidated samples was performed on LEO1455 VP (Zeiss, Germany) scanning electron microscope with blocks of INCA Energy-300 X-ray energy spectrometer.

X-ray phase analysis was performed on Shimadzu XRD-6000 diffractometer in the following modes:

- $\text{CuK}\alpha$ : radiation with  $\lambda=1.54187\ \text{\AA}$ ;
- curved graphite monochromator in front of the counter;
- method  $\theta$ – $2\theta$  of continuous scanning;
- scanning speed:  $1.2^\circ/\text{min}$ ;
- angular range:  $2\theta=5.0$ – $100.0^\circ$  at a step of  $0.02^\circ$ ;
- voltage on the X-ray tube:  $40\ \text{kV}$ ;
- current:  $30\ \text{mA}$ ;
- without rotation of the sample.

Phase analysis of samples was performed using the ASTM database.

Values of microhardness and crack resistance were determined by measuring diagonal of imprint and length of radial cracks. They were obtained by pressing with a diamond indenter [20] having the shape of a quadrilateral pyramid with the angle at the vertex  $\alpha=136^\circ$  (Vickers pyramid) using AFFRI DM8 automatic microhardness tester.

Microhardness was calculated by the following expression [21]:

$$H_v = \frac{k \cdot P_\sigma}{(2 \cdot a)^2}, \quad (1)$$

where  $k$  is the coefficient depending on the indenter shape:  $k=1.854$  for the Vickers pyramid;  $P$  is the indenter load, kg;  $2 \cdot a$  is the average value of the length of both diagonals of the imprint,  $\mu\text{m}$ .

The fracture toughness coefficient characterizing crack resistance of the sample was determined by expression [22]:

$$K_{IC} = 0.016 \cdot \left(\frac{l}{a}\right)^{-0.5} \cdot \left(\frac{H_v}{E \cdot F}\right)^{-0.4} \cdot \frac{H_v \cdot a^{0.5}}{F}, \quad (2)$$

provided

$$0.25 \leq \frac{l}{a} \leq 2.5, \quad (3)$$

where  $H_v$  is microhardness, GPa;  $E$  is Young's modulus, GPa;  $F$  is a constant,  $F \approx 3$ ;  $l$  is the length of the crack from the corner of Vickers pyramid imprint, m;  $a$  is semi-diagonal of the Vickers pyramid imprint, mean distance from the imprint center to the crack end, m.

The bending strength of the sample under conditions of three-point bending was determined by the expression [23]:

$$\sigma_b = \frac{3 \cdot P \cdot L}{2 \cdot b \cdot h^2}, \quad (4)$$

where  $P$  is the force magnitude at the time of the sample division into parts, N;  $L$  is the sample length, mm;  $b$  is the sample width, mm;  $h$  is the sample thickness in the direction parallel to the direction of force applied to the sample, mm

## 5. The results of the study of obtaining composite materials with high physical, mechanical, and operational properties

### 5.1. Microstructure of composite materials based on chemically synthesized zirconium nanopowders

The main characteristics of the microstructure of the polycrystalline material in general, and ceramics in particular, include the size and morphology of grains, size and morphology of pores, and distribution of admixtures. Moreover, to improve the strength properties of the material, special attention should be paid to its porosity nature [24, 25]. Besides the dependence of porosity on electroconsolidation temperature, the morphology of original powders, as well as the formation of pores of various configurations, cause high porosity values. For convenience and compactness of presenting the further analysis, samples of different compositions were marked as in Table 1.

Table 1

Marking of the studied compositions

Composition marking	ZrO <sub>2</sub> powder type
P-1	Spray drying, spherical shape, $d_{av}=70$ nm (NANOE Company, France)
P-2	Deposition from fluoride salts, disc-shaped, $d_{av}=80$ nm (Institute of Monocrystals, Kharkiv, Ukraine)
P-3	Chemical deposition, spherical shape, $d_{av}=10$ nm (I.M. Frantsevich Institute for Problems of Materials Science, Kyiv)

For example, spherical porosity the most acceptable from the point of view of predicting high characteristics of strength properties was found in samples obtained from nanopowders with grain shape close to isodiametric one (P-1 and P-3). In the samples of these powders, spherical particles remained mostly separated and formed only a few aggregates, up to 280 nm in size. The Scaly (disc-shaped) shape of P-2 powders and a certain presence (up to 15%) of irregularly shaped particles (thin films and fragments of spheres) caused a decrease in relative density of samples to 96%. In addition, the formation of coarse intergranular porosity was observed. This type of porosity is not known to delay crack propagation as the pores have sharpening at the grain boundaries with tip configurations similar to those of the primary sharp cracks. This is observed in contrast to the more acceptable spherical (intragranular) porosity which is more likely to delay crack propagation through its local blunting in places where the crack is crossing the pore.

Fig. 3 shows the Vickers pyramid imprints obtained at the same load of 10 N in samples made from powders of the same composition (ZrO<sub>2</sub>-10 wt. % Al<sub>2</sub>O<sub>3</sub>) and different morphology. It is obvious that the nature of the structure and pores formed in the sample made from the powder with a spherical shape of grains (P-1 and P-3) restrains the formation of Palmquist cracks. This contrasts with the structure of the sample prepared from scaly and fragmentary

powders (P-2) in which cracks occur at all imprint vertices at the same load.

Dependence of change in relative density of the studied samples on sintering temperature (Fig. 4) shows that the total density level for all powders increases with increasing of electroconsolidation temperature. Only for P-3, an increase in density is inversely related to alumina concentration. That is, a maximum density of 0.99 was obtained for samples with adding 10 wt. % alumina at 1,250 °C while the density of samples with 20 and 30 wt. % of alumina was 0.97 and 0.89, respectively, at the same temperature (Fig. 4, a).

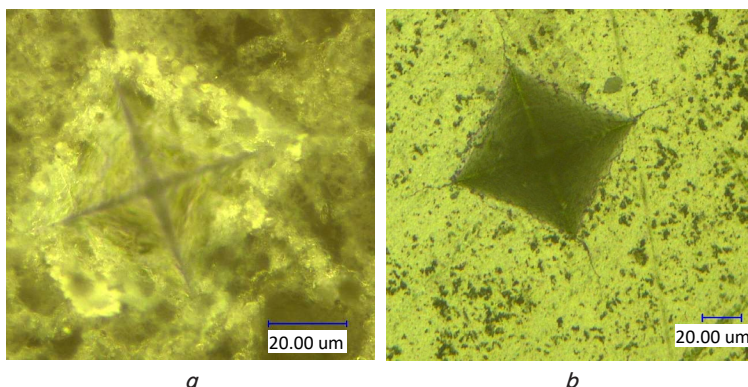


Fig. 3. General view of the imprint and propagation of cracks obtained at a load of 10 N: *a* – in the sample P-2 of composition ZrO<sub>2</sub>-10 wt. % Al<sub>2</sub>O<sub>3</sub>; *b* – sample P-3 of composition ZrO<sub>2</sub>-10 wt. % Al<sub>2</sub>O<sub>3</sub>

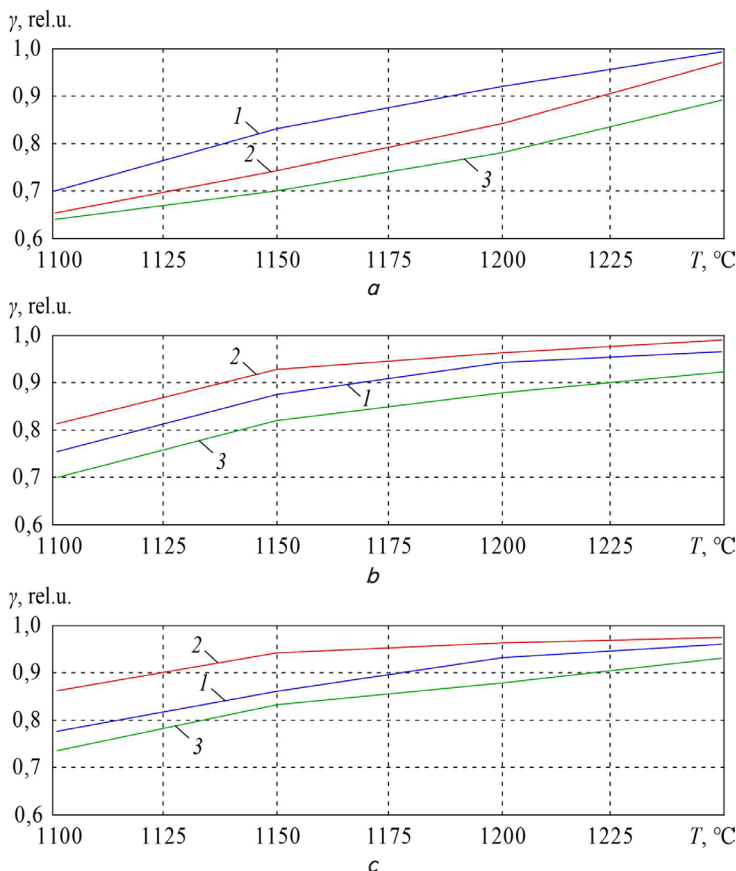


Fig. 4. Dependence of relative density  $\gamma$  on powder sintering temperature  $T$ : *a* – sample of composition P-3; *b* – sample of composition P-2; *c* – sample of composition P-1; 1 – sample with the addition of 10 wt. % Al<sub>2</sub>O<sub>3</sub>; 2 – sample with the addition of 20 wt. % Al<sub>2</sub>O<sub>3</sub>; 3 – sample with the addition of 30 wt. % Al<sub>2</sub>O<sub>3</sub>

The P-2 and P-1 based samples (Fig. 4, *b* and Fig. 4, *c*, respectively) had relative density above 0.7 already at 1100 °C and a steep rise of the curves expressing the dependence of relative density on temperature also indicates better compaction of powders. However, at the same time, this fact does not allow us to obtain P-1 samples and relative density above 0.93. In addition, homogeneous packaging of “soft” agglomerates in initial powders P-2 and P-3 during their compaction contributes to homogeneous packaging of particles in the sample and its compaction during sintering to almost theoretical density.

### 5.2. The effect of additives on structure and properties of materials based on zirconium dioxide nanopowder

Samples prepared on the basis of zirconium nanopowders of different morphologies with alumina additives consolidated at different temperatures were investigated using SEM. It was found that grain size in P-1 samples prepared at temperatures above 1,200 °C is much higher than in the samples prepared from P-2 and P-3 nanopowders at the same temperatures. It is known [26] that aggregation of powder particles is superimposed on the process of growth of interparticle contacts at the expense of other processes, namely coalescence and coagulation each taken separately is capable of predominating over the other in the sintering process. Apparently, the coagulation process in P-1 had a greater influence on the system compaction. This is confirmed by the images of the sample microstructure presented in Fig. 5. The images show that particles are sticking together with the formation of primary, and in some cases, secondary aggregates in which particles do not lose their individuality. There are pores between particles in some places because of insufficient compacting pressure (40 MPa).

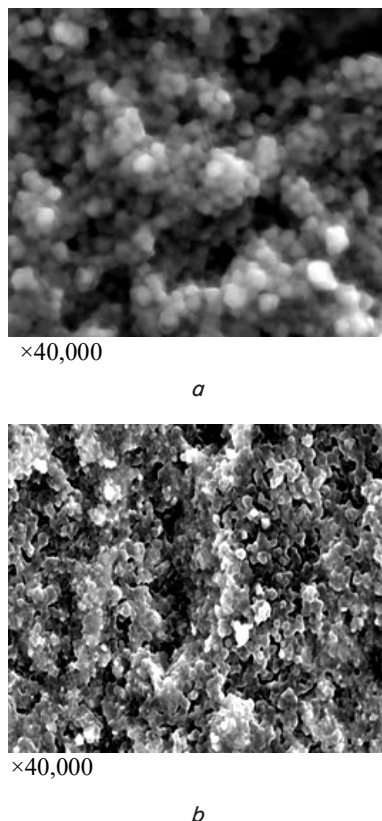


Fig. 5. Microstructure of ceramic samples prepared from P-1 powder: *a* – composition  $ZrO_2$ ; *b* – composition  $ZrO_2$ –10 wt. %  $Al_2O_3$

The coalescence process is characteristic of P-2 and P-3 powder samples and competes with the shrinkage process at the initial stage of consolidation. During electric sintering, shrinkage activation is provided by heating the workpiece with an industrial frequency current. This leads to a significant reduction in yield strength, and hence, obtaining a denser material at the same pressure. This feature is associated with the intensification of grain boundary diffusion [27] which results in the predominance of compaction processes over the processes of ceramic grain growth due to the removal of open pores. It is known that the change in heating rate leads to an increase in the temperature gradient inside the powder being sintered and creating a local mismatch of thermal expansion coefficients [28, 29]. Besides, a significant discrepancy between the coefficients of thermal expansion of zirconium oxide and alumina powder particles leads to dislocations motion to the boundaries being formed raising their free volume and grain boundary diffusion coefficient.

### 5.3. Establishment of the optimal composition of initial mixtures and sintering modes using alumina nano additives

Analysis of the relationship between the structure of obtained samples, consolidation regimes, and final density has shown that temperature rise leads to rapid grain growth. Larger grains are characteristic of the samples obtained at elevated sintering temperatures (Fig. 6) under the condition of applying maximum pressure at the stage of holding. It became obvious that a temperature of 1,200 °C is sufficient to achieve at least a 97 % relative density. The grain size remains less than 300 nm (Fig. 6, *a*). However, it was necessary to provide such a value of density at the initial stage that would be enough to achieve a uniform distribution of porosity alongside the obvious advantage of reducing the consolidation temperature to 1,200 °C. It became possible to achieve only by consolidating the P-3 powder with composition  $ZrO_2$ –10 wt. %  $Al_2O_3$  at 1,200 °C (Fig. 6, *d*).

At proximity of scales, fracture structure in samples prepared from P-2 and P-3 powders (Fig. 7, *a*, *b* and Fig. 7, *c*, *d*, respectively) was almost the same but there were some differences in their nature. Areas with micro pits are visible on the surface of fracture of the sample prepared from P-2 powder (Fig. 8). Probably, these pits have appeared as a result of the formation and fusion of microvoids near elongated structural inhomogeneities [30] as well as in places of formation of large pores that are tapering at the grain boundaries.

In addition, since a large proportion of this powder's particles are almost flat scales, there are a number of pores between two almost flat surfaces. This leads to processes of zonal separation which are usually decisive in the sintering of fine powders [31, 32].

The appearance of fracture in ceramics of P-3 powder consolidated at different temperatures in the range of 1,150–1,250 °C taken from samples with a relative density of more than 98 % (Fig. 9) is characterized by a morphologically uniform fracture surface. That is, it has no noticeable geometric areas. At a consolidation temperature of 1,150 °C (Fig. 9, *a*), chips from this sample were homogeneous, with almost imperceptible boundaries between grains and average pore size of about 190 nm. As the consolidation temperature increases, the average grain size increases with a simultaneous decrease in pore size to 150 nm. Along with well-“drawn” grain boundaries in the sample baked at 1,200 °C (Fig. 9, *b*), elements of microrelief of rectilinear fracture (stepwise) are distinguished (Fig. 9, *c*). They can occur as a result of splitting along the boundaries of twins [33, 34].

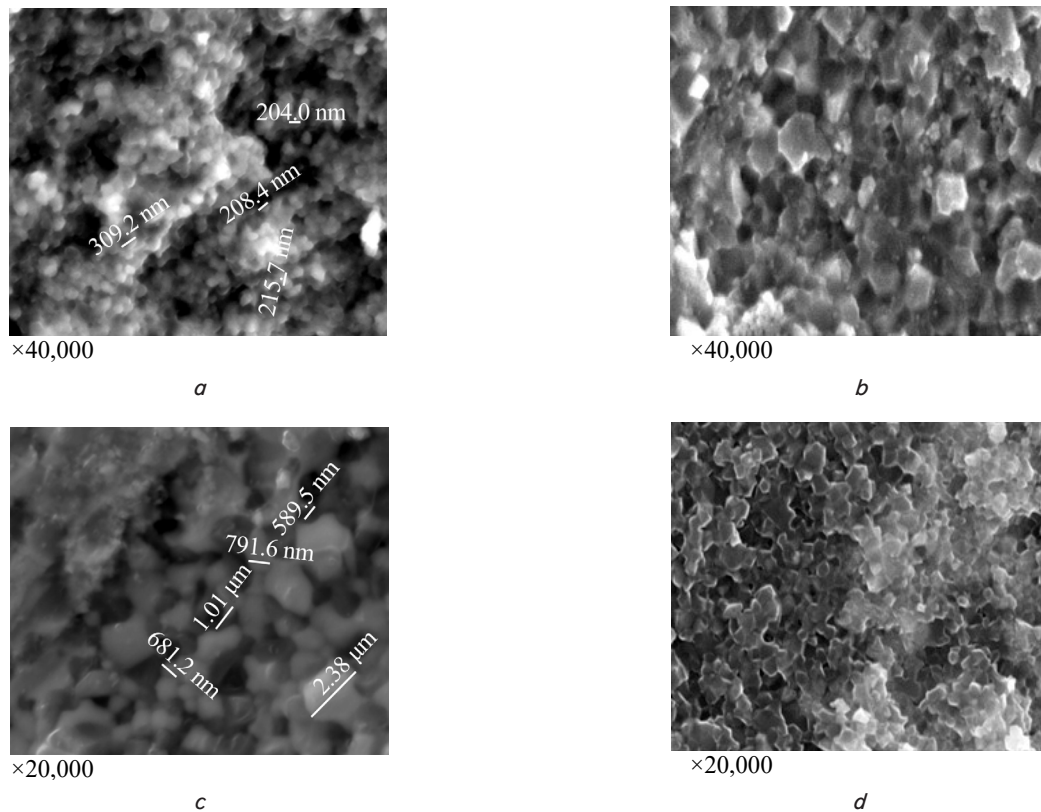


Fig. 6. Microstructure of ceramics with composition  $ZrO_2-10 \text{ wt. } \% Al_2O_3$ : *a* – the sample of P–2 powder sintered at 1,220 °C; *b* – the sample of P–2 powder sintered at 1,250 °C; *c* – the sample of P–2 powder sintered at 1,300 °C; *d* – the sample of P–3 powder sintered at 1,200 °C

It was also noted in [33] that the presence of areas with twin relief in the fracture surface may be an evidence of the occurrence of a tetragonal-monoclinic transition in the material during its fracturing. The presence of much larger pores (above 100 nm) was noted in fragments of the samples sintered at 1,250 °C (Fig. 9, *c*) while the inside size of the agglomerated pores was reduced. Moreover, the sample density did not change, i.e. the overall pore volume remained the same. All this can reduce macroscopic shrinkage which is confirmed by analysis of the shrinkage curve for a sample with the addition of 10 wt. % alumina.

The structure of chips taken from samples prepared from P–1 powder was less homogeneous. In contrast to the samples prepared from P–3 powder, samples of the above powders (with the lowest density) examined at high magnification ( $\times 20,000$ ) had not only coarser grains (Fig. 10, *a*) but also the fracture nature. Chipping in this case occurs along the boundaries of grains (agglomerates) with a stream-like pattern (Fig. 10, *b*) which may also indicate instability of boundaries [35].

Particles prepared of P–2 powder were slightly sticky and, in contrast to spheroidized particles (P–1 and P–3 powders), had low fluidity. As a result, air that was incompletely displaced from the material interacted with the carbon of the graphite mold, and CO was formed. This was manifested by characteristic odor of organic impurities in the elongated sample which in turn caused powder burnout during sintering. In this regard, a coefficient was introduced when dosing the powder to take into account the powder

loss during sintering:  $K=1.01$ . Besides, according to the data of chemical analysis of samples (Fig. 11, Tables 2, 3), in addition to the main elements (Y, Zr, O), the samples contained adsorbed oxygen and carbon which enter the CH, C–O, and COOH groups [36].

Table 2

The results of chemical analysis of samples prepared from P–2 powder:  $ZrO_2-10 \text{ wt. } \% Al_2O_3$  composition

Spec-trum	Statistical analysis of element distribution	C	O	Al	Y	Zr	Total
		in wt. %					
1	Yes	3.24	24.39	0.84	0.23	71.31	100.00
2	Yes	5.10	23.67	0.42	0.95	69.86	100.00
3	Yes	3.31	23.88	1.49	1.06	70.27	100.00
4	Yes	1.79	23.78	0.43	0.81	73.19	100.00
5	Yes	6.39	22.72	0.55	2.53	67.81	100.00
6	Yes	6.84	22.80	0.26	2.12	67.98	100.00
7	Yes	6.45	22.21	0.49	2.84	68.00	100.00
8	Yes	5.37	23.47	2.46	2.81	65.89	100.00
9	Yes	3.08	24.88	0.99	1.22	69.84	100.00
10	Yes	5.33	23.87	1.28	2.53	66.99	100.00
Mean deviation		4.69	23.57	0.92	1.71	69.11	100.00
Standard deviation		1.72	0.80	0.67	0.96	2.18	–
Maximal deviation		6.84	24.88	2.46	2.84	73.19	–
Minimal deviation		1.79	22.21	0.26	0.23	65.89	–
Data of the reference material described in [37]		2.50	24.90	0.90	0.24	71.46	100.00

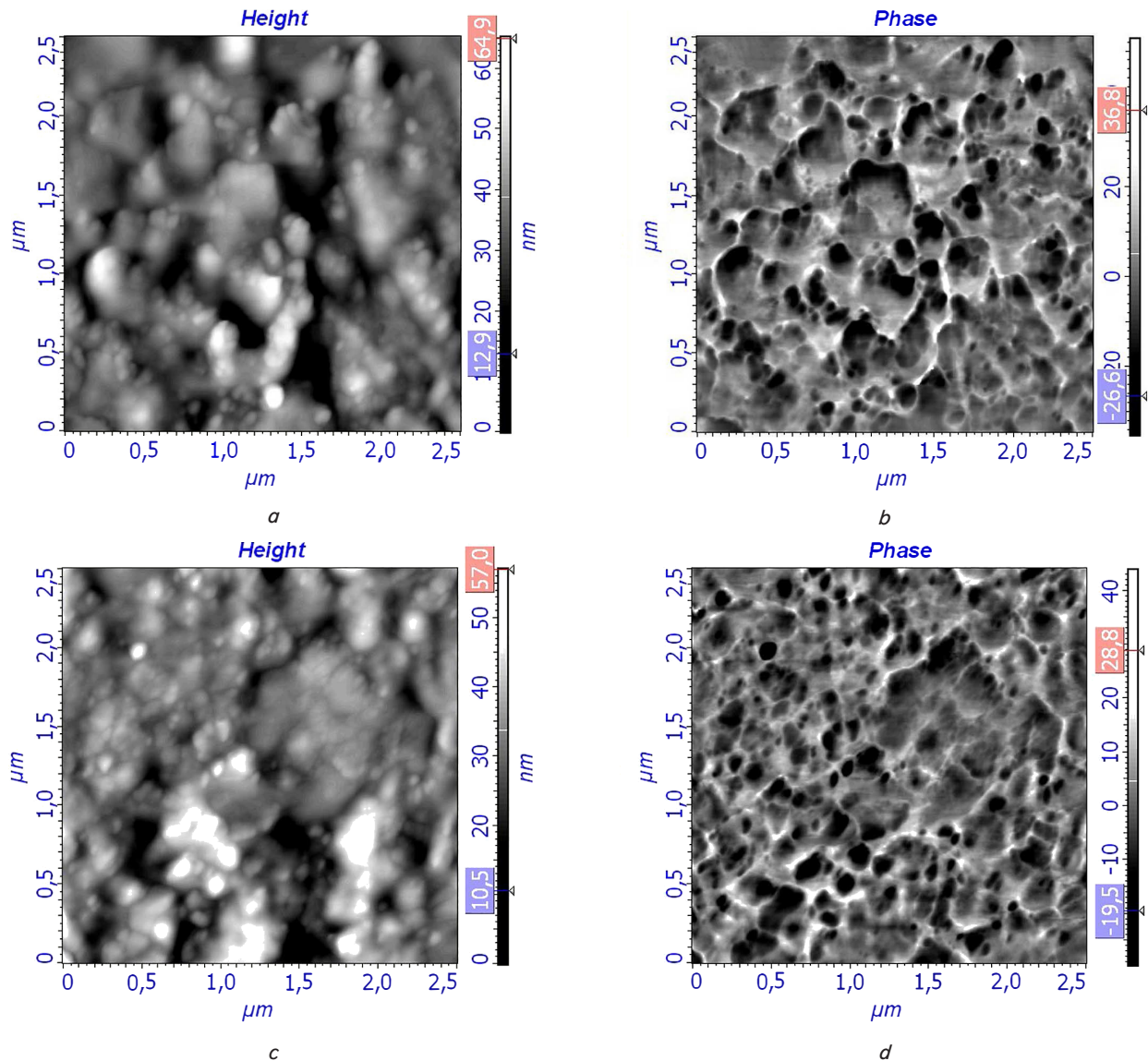


Fig. 7. AFM image of chips from samples with  $ZrO_2-30 \text{ wt. \% } Al_2O_3$  composition sintered at  $1,200 \text{ }^\circ C$ : *a* – fracture height in samples prepared from P–2 powder; *b* – structure of fracture in samples prepared from P–2 powder; *c* – fracture height in samples prepared from P–3 powder; *d* – structure of fracture in samples prepared from P–3 powder

Table 3

The results of chemical analysis of samples prepared from P–2 powder:  $ZrO_2-30 \text{ wt. \% } Al_2O_3$  composition

Spectrum	Statistical analysis of element distribution	in wt. %						Total
		C	O	Al	Y	Zr		
1	Yes	0.92	45.62	50.71	0.67	2.07	100.00	
2	Yes	3.33	45.81	37.23	0.85	12.78	100.00	
3	Yes	2.61	46.23	43.14	0.00	8.03	100.00	
4	Yes	4.31	45.73	39.25	0.29	10.42	100.00	
5	Yes	2.63	45.60	48.39	0.00	3.39	100.00	
6	Yes	2.41	46.23	35.60	0.00	15.75	100.00	
Mean deviation		2.70	45.87	42.39	0.30	8.74	100.00	
Standard deviation		1.12	0.29	6.14	0.38	5.33	–	
Maximal deviation		4.31	46.23	50.71	0.85	15.75	–	
Minimal deviation		0.92	45.60	35.60	0.00	2.07	–	

with a relative density of 81 % ( $ZrO_2$ ) and 86 % ( $ZrO_2-20 \text{ wt\% } Al_2O_3$ ), respectively. However, there was a significant growth of grains up to 580 nm and merging of individual grains into up to 950 nm agglomerates (Fig. 12).

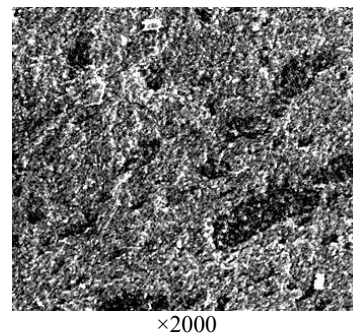
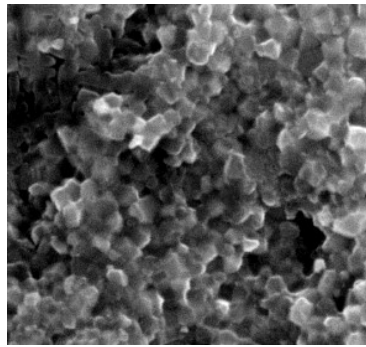


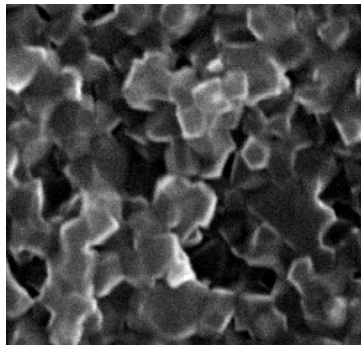
Fig. 8. Structure of fracture in the sample with  $ZrO_2-20 \text{ wt. \% } Al_2O_3$  composition prepared from P–2 powder sintered at  $1,250 \text{ }^\circ C$

It should be noted that common sintering at  $1,500 \text{ }^\circ C$  and holding time of 1 hour for samples of pure P–1 powder and with the addition of 20 wt. %  $Al_2O_3$  allowed us to obtain a material



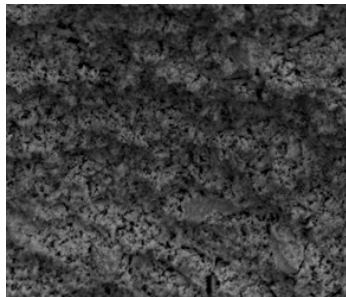
×15,000

*a*



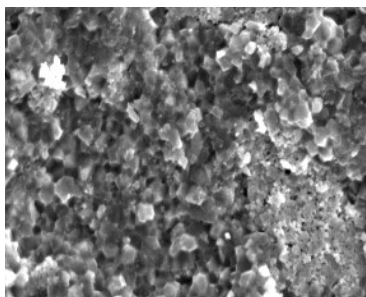
×25,000

*b*



×5000

*c*

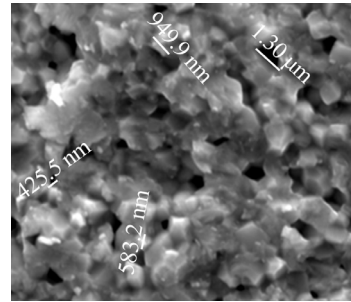


×10,000

*d*

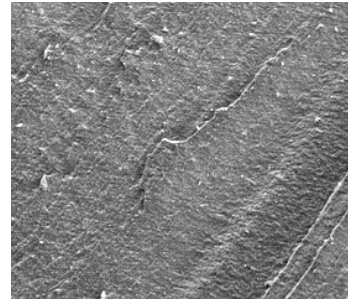
Fig. 9. Microstructure of chips taken from samples of  $ZrO_2-10$  wt. %  $Al_2O_3$  composition obtained from P-3 powder sintered at temperature: *a* – 1,150 °C; *b*, *c* – 1,200 °C; *d* – 1,250 °C

Besides, sintering was accompanied by significant sample shrinkage: a 40 % decrease in volume from the volume of the pre-compressed compact.



×20,000

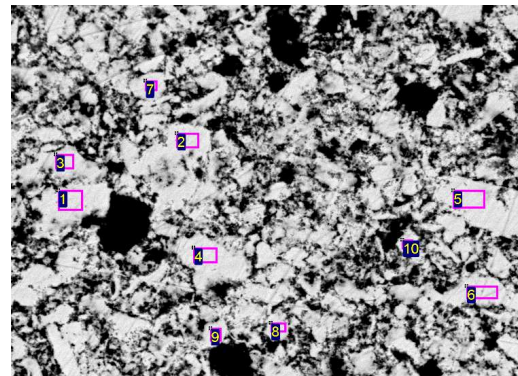
*a*



×1000

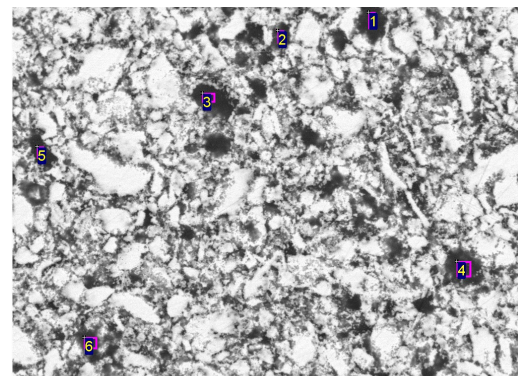
*b*

Fig. 10. Microstructure of chips taken from samples of  $ZrO_2-20$  wt. %  $Al_2O_3$  composition prepared from P-1 powder: *a* – inhomogeneity of the sample chip structure; *b* – stream-like pattern nature of the sample fracture



20 μm

*a*



20 μm

*b*

Fig. 11. The results of chemical analysis of samples prepared from P-2 powder: *a* –  $ZrO_2-10$  wt. %  $Al_2O_3$  composition; *b* –  $ZrO_2-30$  wt. %  $Al_2O_3$  composition

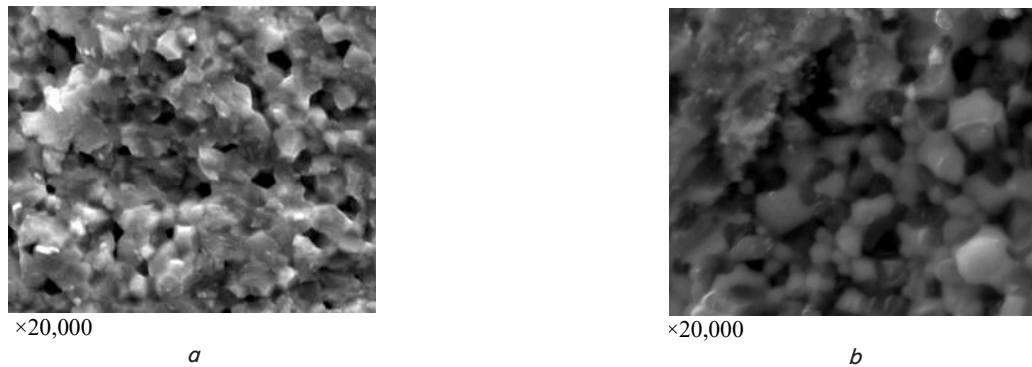


Fig. 12. Microstructure of samples prepared from P-1 powder: *a* – ZrO<sub>2</sub> composition; *b* – ZrO<sub>2</sub>-20 wt. % Al<sub>2</sub>O<sub>3</sub> composition

**5. 4. Forecasting the possible ways to improve properties of composite materials based on zirconium dioxide**

Analysis of phase composition, along with morphology and dispersion of powders, makes it possible to predict the performance of products at the initial stage of material production [37, 38]. When examining radiographs taken from the polished surface of consolidated samples of ZrO<sub>2</sub>-Al<sub>2</sub>O<sub>3</sub> ceramics, it was found that phase composition is characterized by the presence of peaks of monoclinic, tetragonal zirconium dioxide and alumina in different ratios. This depends on electroconsolidation temperature and the amount of alumina in the initial powder mixtures [39, 40]. The following can be seen when examining radiographs of the samples obtained by hot pressing at 1,200 °C with the transmission of high-ampere current at various alumina contents:

- content of the monoclinic phase increased with an increase in Al<sub>2</sub>O<sub>3</sub> content from 10 wt. % (Fig. 13) to 20 wt. % (Fig. 14);
- content of the monoclinic phase in the sample (Fig. 15) obtained at 1,250 °C was reduced to almost zero at Al<sub>2</sub>O<sub>3</sub> content of 30 wt. %

Some researchers [41, 42] believe that the composite strength should decrease with an increase in monoclinic phase content because the volume of the monoclinic phase is greater than the volume of the tetragonal phase. It is obvious that the growth of forces in the composite volume increases internal stresses of the system and this, ultimately, reduces the material strength [43, 44]. In the case under study, this did not happen due to the influence of additives of alumina nanopowders which slightly distorts the crystal structure of tetragonal zirconium oxide resulting in its growth. This compensated for the monoclinic phase pressure.

The presence of a large quantity of monoclinic phase indicates the polymorphic conversion of tetragonal zirconium dioxide into a low-temperature modification during cooling. The partial conversion could also be facilitated by the low cooling rate of the samples which, according to [45], does not

contribute to the fixation of high-temperature phases. This fact can give an advantage in the rate of sample sintering due to the fact that the polymorphic transformation contributes to this phenomenon.

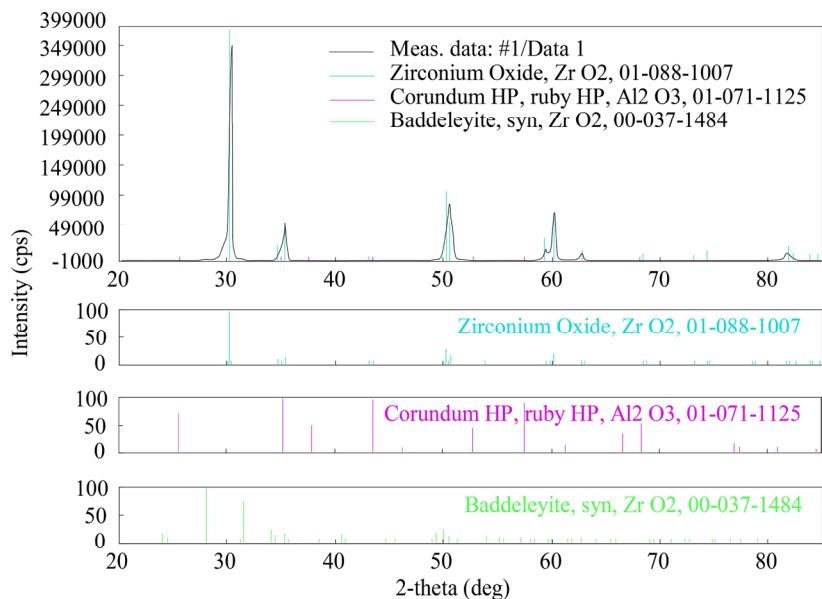


Fig. 13. Radiograph of the polished surface of the sample sintered at 1,250 °C containing 10 wt. % Al<sub>2</sub>O<sub>3</sub>

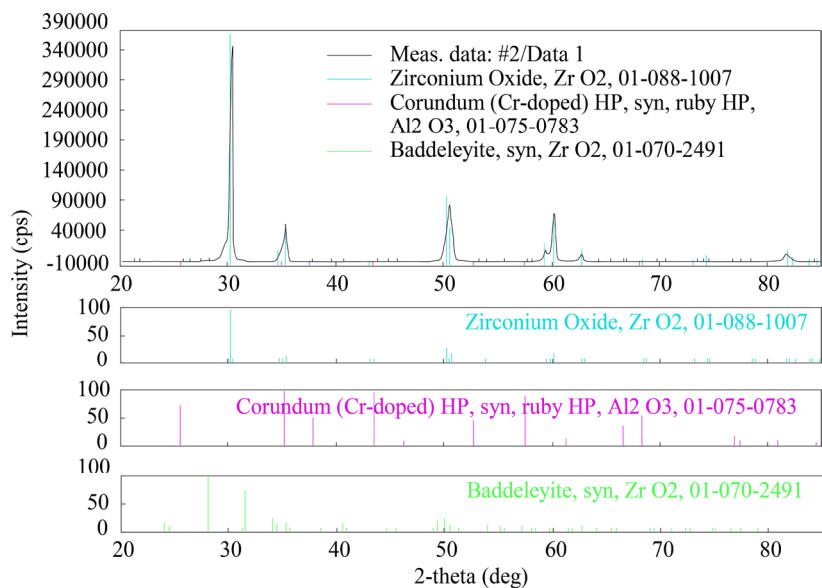


Fig. 14. Radiograph of the polished surface of the sample sintered at 1,250 °C containing 20 wt. % Al<sub>2</sub>O<sub>3</sub>

It is known that in addition to external energy sources (electric current), the appearance of additional internal heat sources (polymorphic transformation occurs with a release of heat) reduces temperature and accelerates the sintering process [46].

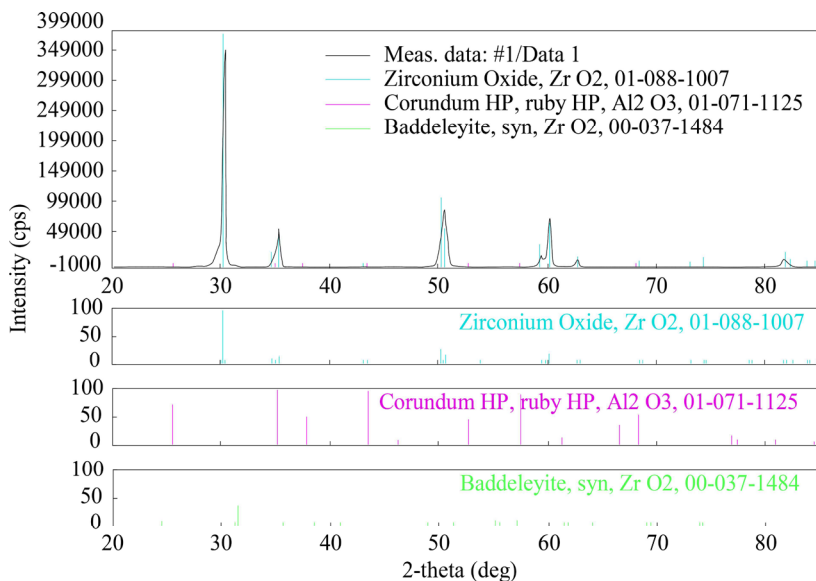


Fig. 15. Radiograph of the polished surface of the sample obtained at 1,250 °C containing 30 wt. %  $\text{Al}_2\text{O}_3$

We can assume a significant crystallite and porosity growth at 1,250 °C as well as the presence of stresses initiated by tetragonal-monoclinic transformation. This destroys crystallites of the tetragonal zirconium dioxide phase and leads to a decrease in their number in solid solution  $(\text{ZrO}_2)_{0.97}(\text{Y}_2\text{O}_3)_{0.03}$  [47].

Thus, the gain in the sintering rate does not provide an advantage in obtaining an acceptable fine-grained structure. The effect of alumina at the retention of up to 30 wt. % also means that the monoclinic phase is completely transformed into a tetragonal one. This can be explained by the fact that temperature rises rapidly under the influence of high-ampere electric current in the process of hot pressing and partially stabilized zirconium dioxide begins to conduct current through ion mobility as soon as 800 °C is reached [48].

Passage of high-ampere current significantly activates the sintering process contributing to the grain-boundary slip of alumina nanopowders and complete transformation of the monoclinic phase of zirconium dioxide into tetragonal one [49, 50]. In fact, zirconium oxide becoming permeable as the temperature rises obviously contributes to the percolation effects when an electric current is passed. Electric current promotes the surface activity of nanopowders and its variable value promotes partial crushing of agglomerated grains, thus affecting structure formation in composites.

Naturally, the structure is affected by the final sintering temperature. It should be noted that the increase in sintering temperature also decreases the content of the monoclinic phase which turns into a tetragonal phase. The radiograph of the test sample containing 30 wt. %  $\text{Al}_2\text{O}_3$

(Fig. 16) obtained at 1,250 °C had reflections belonging only to the tetragonal zirconium oxide. Since the cooling time did not depend on alumina concentration in the starting powder, the amount of tetragonal  $\text{ZrO}_2$  in the test sample increased with the increasing concentration of  $\text{Al}_2\text{O}_3$  in initial powders.

It is interesting to note that the phase composition of this sample fracture is characterized by the presence of low-intensity peaks of monoclinic zirconium oxide and the fracture surface has domains of intergranular fracture inherent in the presence of a low-temperature phase [51]. These facts indicate that there is a tetragonal-monoclinic transformation during loading. That is, admixtures of 30 wt. % of alumina contribute to the strengthening of the material based on zirconium oxide while inhibiting abnormal growth of grains and formation of a finer structure with a high content of tetragonal phase. The tetragonal phase is capable of transforming into a monoclinic phase (under the action of stresses) near the crack tip.

Table 4 shows the mechanical properties of some samples of powders P-1 and P-2 obtained at different temperatures, the pressure of 30 MPa, and the holding time of 3 min.

Table 2 shows that the mechanical properties of the composite material improve with an increase in temperature and quantity of  $\text{Al}_2\text{O}_3$  nanopowder additives. Mechanical properties, in particular crack resistance, approach the properties of the material based on the NANO brand powder at a temperature of 1,250 °C in the composite material based on synthesized zirconium dioxide.

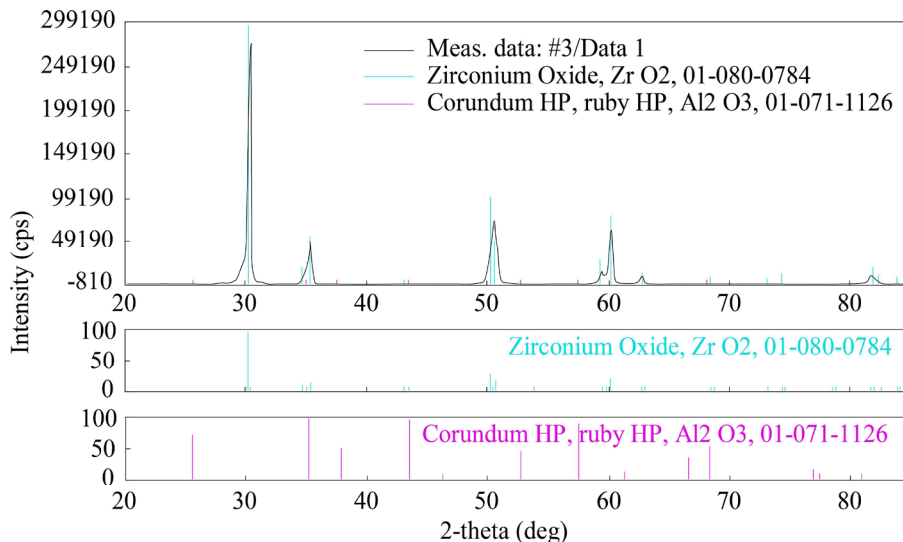


Fig. 16. Radiograph of the polished surface of the sample containing 30 wt. %  $\text{Al}_2\text{O}_3$  obtained at 1,250 °C

Table 4

Mechanical properties of various sintered samples

Sample composition	Temperature, °C	Density, g/cm <sup>3</sup>	Hardness, GPa	Crack growth resistance, MPa m <sup>1/2</sup>	Flexural strength, MPa
P-1 powder of ZrO <sub>2</sub> -10 wt. % Al <sub>2</sub> O <sub>3</sub> composition	1,150	5.45	12.5±0.15	7.2±0.2	802±25
P-1 powder of ZrO <sub>2</sub> -20 wt. % Al <sub>2</sub> O <sub>3</sub> composition	1,200	5.49	12.5±0.12	7.5±0.2	805±10
P-1 powder of ZrO <sub>2</sub> -30 wt. % Al <sub>2</sub> O <sub>3</sub> composition	1,250	5.54	13.2±0.15	7.8±0.4	850±25
P-2 powder of ZrO <sub>2</sub> -10 wt. % Al <sub>2</sub> O <sub>3</sub> composition	1,150	5.32	12±0.2	7.10±0.15	780±15
P-2 powder of ZrO <sub>2</sub> -20 wt. % Al <sub>2</sub> O <sub>3</sub> composition	1,200	5.40	12.5±0.15	7.15±0.15	810±10
P-2 powder of ZrO <sub>2</sub> -30 wt. % Al <sub>2</sub> O <sub>3</sub> composition	1,250	5.53	13±0.15	7.8±0.23	830±10

## 6. Discussion of the results obtained in the study of structure formation in the composites based on synthesized nanopowders of zirconium dioxide

Studies have shown that the microstructure of the samples in which zirconium dioxide was obtained in different ways strongly depends on tetragonal-monoclinic transitions. For example, the nature of the structure and pores formed in the samples prepared of powder with composition ZrO<sub>2</sub>-10 wt. % Al<sub>2</sub>O<sub>3</sub> with grains of spherical shape (Fig. 3, *b*) inhibit the formation of Palmquist cracks at the same load of 10 N. This is in contrast to the structure in a sample prepared of powders of the scaly-fragmental form (Fig. 3, *a*) in which cracks occur at all vertices of the Vickers pyramid imprint at the same load. A maximum density of 0.99 was obtained for samples with 10 wt. % Al<sub>2</sub>O<sub>3</sub> additives at 1,250 °C (Fig. 4, *a*) while the density of the samples with 20 and 30 % Al<sub>2</sub>O<sub>3</sub> additives was 0.97 and 0.89, respectively, at the same temperature.

In samples from P-1 powder obtained at temperatures above 1,200 °C, grains were much coarser than in the samples obtained from P-2 and P-3 nanopowders at the same temperature. The coagulation process in P-1 powder had a greater influence on the system compaction which is confirmed by images of the sample microstructure (Fig. 5). Sticking of particles occurs with the formation of primary and secondary aggregates (in some cases) in which particles have not lost their individuality. There are pores between particles in some places because of insufficient compacting pressure (40 MPa). Significant discrepancy between the coefficients of thermal expansion of zirconium oxide and alumina powder particles led to the motion of dislocations to the boundaries being formed increasing their free volume and the coefficient of grain boundary diffusion.

Chemical analysis of the samples has shown that the increase in the content of nano additives of alumina Al<sub>2</sub>O<sub>3</sub> from 10 wt. % (Table 2) to 30 wt. % (Table 3) improved strength and crack resistance (Fig. 11). At the same time, there was a restraint of abnormal grain growth and formation of a finer structure at high content of tetragonal phase. Sintering of samples of pure P-1 powder and samples with

addition of 20 wt. % Al<sub>2</sub>O<sub>3</sub> at 1,500 °C has allowed us to obtain a material with a relative density of 81 % (ZrO<sub>2</sub>) and 86 % (ZrO<sub>2</sub>-20 wt. % Al<sub>2</sub>O<sub>3</sub>). There was a significant growth of grains, up to 580 nm, and individual grains formed agglomerates of up to 950 nm size (Fig. 12).

Radiographs of the samples obtained by hot pressing at 1,200 °C with the transmission of high-ampere electric current have shown the following. Content of the monoclinic phase increased with increasing Al<sub>2</sub>O<sub>3</sub> content from 10 wt. % (Fig. 13) to 20 wt. % (Fig. 14). At a content of 30 wt. % Al<sub>2</sub>O<sub>3</sub> in the sample (Fig. 15) obtained at 1,250 °C, the content of the monoclinic phase was reduced to almost zero. To further improve the mechanical properties of the samples, the sintering temperature and holding time can be increased because grain growth at 30 % alumina content was not as fast as at lower values. It is assumed that the combination

of various nano additives of other types, along with alumina, will further increase the physical and mechanical properties of the resulting composites.

The study limitation consists in that thermogravimetric studies have not been performed completely during sintering with various additives. Besides, not all samples were tested for mechanical strength and comparison of mechanical properties with materials produced by worldwide known manufacturers was made not in full.

It would be appropriate to achieve greater grain dispersion in further studies and reduce the content of residual additives resulting from the use of chemical processes of composite production.

## 7. Conclusions

1. Microstructure of composite materials based on chemically synthesized zirconium dioxide nanopowders obtained by the electroconsolidation has been studied. It was found that the microstructure of the samples in which zirconium dioxide was obtained in different ways strongly depends on tetragonal-monoclinic transitions.

2. Regularities of the effect of additives, in particular alumina, on the structure and physical and mechanical properties of composite materials based on specifically synthesized zirconium dioxide nanopowder were revealed, phase composition of the obtained nanocomposites and their features were determined. For example, an increase in the content of alumina nano additives up to 30 wt. % helps to increase the strength and crack resistance of the samples made of the material based on zirconium oxide. At the same time, there is a restraint of abnormal grain growth and formation of a finer structure with a high content of tetragonal phase.

3. Optimal composition of initial mixtures and sintering modes using alumina nano additives was established in order to improve the physical and mechanical properties of the material. To improve the mechanical properties of the samples, sintering temperature and holding time can be raised because alumina grain growth is less rapid at a 30 % content than at lower contents.

4. Based on the conducted studies, a forecast was made concerning possible ways of improving the properties of composite materials with a fine microstructure obtained by using zirconium dioxide. As the temperature and amount of  $\text{Al}_2\text{O}_3$  nanopowder additives increase, the mechanical properties of the composite material improve. Mechanical properties, in particular crack resistance, in the composite material based on the synthesized zirconium dioxide approached at  $1,250^\circ\text{C}$  the properties of the material based on NANO brand powder. This will contribute to the fact that zirconium oxide obtained by chemical decomposition from fluoride salts and having crack resistance of  $7.8\text{ MPa}\cdot\text{m}^{1/2}$

at a strength of 820 MPa will be quite competitive with the currently known imported analogs.

---

### Acknowledgments

---

The article was prepared as part of a study under the state budget topic The Use of Non-traditional Methods of Obtaining Nanopowders and Sintering in the Development of Modified Mullite-ZrO<sub>2</sub> Ceramics Resistant to Heat Shock (State Registration Number 0121U109441) with the financial support of the Ministry of Education and Science of Ukraine.

---

### References

1. Gevorkyan, E. S., Vovk, R. V., Sofronov, D. S., Nerubatskyi, V. P., Morozova, O. M. (2021). The composite material based on synthesized zirconium oxide nanopowder for structural appliance. 17th Edition of Advanced Nano Materials. Aveiro, 267. Available at: <http://repo.knmu.edu.ua/handle/123456789/29324>
2. Von Steyern, P. V., Carlson, P., Nilner, K. (2005). All-ceramic fixed partial dentures designed according to the DC-Zirkon® technique. A 2-year clinical study. *Journal of Oral Rehabilitation*, 32 (3), 180–187. doi: <https://doi.org/10.1111/j.1365-2842.2004.01437.x>
3. Chevalier, J., Gremillard, L., Deville, S. (2007). Low-Temperature Degradation of Zirconia and Implications for Biomedical Implants. *Annual Review of Materials Research*, 37 (1), 1–32. doi: <https://doi.org/10.1146/annurev.matsci.37.052506.084250>
4. Schmitt, J., Goellner, M., Wichmann, M., Reich, S. (2012). Zirconia posterior fixed partial dentures: 5-year clinical results of a prospective clinical trial. *The International journal of prosthodontics*, 25 (6), 585–589. Available at: [https://www.researchgate.net/publication/232706570\\_Zirconia\\_Posterior\\_Fixed\\_Partial\\_Dentures\\_5-Year\\_Clinical\\_Results\\_of\\_a\\_Pro prospective\\_Clinical\\_Trial](https://www.researchgate.net/publication/232706570_Zirconia_Posterior_Fixed_Partial_Dentures_5-Year_Clinical_Results_of_a_Pro prospective_Clinical_Trial)
5. Roe, P., Kan, J. Y. K., Rungcharassaeng, K., Won, J. B. (2011). Retrieval of a Fractured Zirconia Implant Abutment Using a Modified Crown and Bridge Remover: A Clinical Report. *Journal of Prosthodontics*, 20 (4), 315–318. doi: <https://doi.org/10.1111/j.1532-849x.2011.00696.x>
6. Gevorkyan, E. S., Nerubatskyi, V. P., Mel'nik, O. M. (2010). Goryachee pressovanie nanoporoshkov sostava ZrO<sub>2</sub>-5 %Y<sub>2</sub>O<sub>3</sub>. *Zbirnyk naukovykh prats Ukrainkoj derzhavnoi akademiyi zaliznychnoho transportu*, 119, 106–110.
7. Hannink, R. H. J., Kelly, P. M., Muddle, B. C. (2004). Transformation Toughening in Zirconia-Containing Ceramics. *Journal of the American Ceramic Society*, 83 (3), 461–487. doi: <https://doi.org/10.1111/j.1151-2916.2000.tb01221.x>
8. Morozova, O. M., Timofeeva, L. A., Chyshkala, V. A., Gevorkyan, E. S., Nerubatskyi, V. P., Rutskyi, M. (2021). Improvement of metrological support of a new material composition based on zirconium dioxide. Abstracts of the 2nd International Scientific and Technical Conference «Intelligent Transport Technologies». Kharkiv: USURT, 154–155. Available at: <http://repo.knmu.edu.ua/handle/123456789/28604>
9. Chyshkala, V. O., Lytovchenko, S. V., Gevorkyan, E. S., Nerubatskyi, V. P., Morozova, O. M. (2021). Mastering the processes of synthesis of oxide compounds with the use of a powerful source of fast heating of the initial ingredients. *Zbirnyk naukovykh prats Ukrainskoho derzhavnoho universytetu zaliznychnoho transportu*, 196, 118–128. Available at: [https://kart.edu.ua/wp-content/uploads/2021/04/tht\\_zbirn\\_196.pdf](https://kart.edu.ua/wp-content/uploads/2021/04/tht_zbirn_196.pdf)
10. Marek, I. O., Ruban, O. K., Redko, V. P., Danylenko, M. I., Dudnik, O. V. (2017). Nanokrystalichni poroshky na osnovi ZrO<sub>2</sub> dlia vyhotovlennia kompozytiv, stiykykh do protsesu starinnia. *Nanosistemi, Nanomateriali, Nanotehnologii*, 15 (1), 91–98. Available at: [https://www.imp.kiev.ua/nanosys/media/pdf/2017/1/nano\\_vol15\\_iss1\\_p0091p0098\\_2017.pdf](https://www.imp.kiev.ua/nanosys/media/pdf/2017/1/nano_vol15_iss1_p0091p0098_2017.pdf)
11. Sokolov, I. E., Fomichev, V. V., Zakalyukin, R. M., Kopylova, E. V., Kumskov, A. S., Mozhchil, R. N., Ionov, A. M. (2021). Synthesis of nanosized zirconium dioxide, cobalt oxide and related phases in supercritical CO<sub>2</sub> fluid. *Izvestiya Vysshikh Uchebnykh Zavedenii Khimiya Khimicheskaya Tekhnologiya*, 64 (5), 35–43. doi: <https://doi.org/10.6060/ivkkt.20216405.6060>
12. McLaren, E. A., Maharishi, A., White, S. N. (2021). Influence of yttria content and surface treatment on the strength of translucent zirconia materials. *The Journal of Prosthetic Dentistry*. doi: <https://doi.org/10.1016/j.prosdent.2021.07.001>
13. Markandan, K., Chin, J. K., Tan, M. T. T. (2014). Study on Mechanical Properties of Zirconia-Alumina Based Ceramics. *Applied Mechanics and Materials*, 625, 81–84. doi: <https://doi.org/10.4028/www.scientific.net/amm.625.81>
14. Boniecki, M., Sadowski, T., Gołębiewski, P., Węglarz, H., Piątkowska, A., Romaniec, M. et al. (2020). Mechanical properties of alumina/zirconia composites. *Ceramics International*, 46 (1), 1033–1039. doi: <https://doi.org/10.1016/j.ceramint.2019.09.068>
15. Li, Q., Hao, X., Gui, Y., Qiu, H., Ling, Y., Zheng, H. et al. (2021). Controlled sintering and phase transformation of yttria-doped tetragonal zirconia polycrystal material. *Ceramics International*, 47 (19), 27188–27194. doi: <https://doi.org/10.1016/j.ceramint.2021.06.139>
16. Gevorkyan, E. S., Morozova, O. OcM., Sofronov, D. S., Chyshkala, V. A., Nerubatskyi, V. P. (2021). Composite material based on synthesized zirconium oxide nanopowders with enhanced mechanical properties. International workshop for young scientists (IS-MA-2021) «Functional materials for technical and biomedical applications». Kharkiv, 29. Available at: <http://repo.knmu.edu.ua/handle/123456789/29292>
17. Gevorkyan, E. S., Morozova, O. M., Sofronov, D. S., Nerubatskyi, V. P., Ponomarenko, N. S. (2021). The formation of ZrO<sub>2</sub>-Y<sub>2</sub>O<sub>3</sub>-nanoparticles from fluoride solutions. II International Advanced Study Conference Condensed Matter and Low Temperature Physics 2021. Kharkiv: FOP Brovin O. V., 190. Available at: <http://repo.knmu.edu.ua/handle/123456789/28791>

18. Gevorkyan, E. S., Rucki, M., Kagramanyan, A. A., Nerubatskiy, V. P. (2019). Composite material for instrumental applications based on micro powder Al<sub>2</sub>O<sub>3</sub> with additives nano-powder SiC. *International Journal of Refractory Metals and Hard Materials*, 82, 336–339. doi: <https://doi.org/10.1016/j.ijrmhm.2019.05.010>
19. Gevorkyan, E., Nerubatskiy, V., Gutsalenko, Y., Melnik, O., Voloshyna, L. (2020). Examination of patterns in obtaining porous structures from submicron aluminum oxide powder and its mixtures. *Eastern-European Journal of Enterprise Technologies*, 6 (6 (108)), 41–49. doi: <https://doi.org/10.15587/1729-4061.2020.216733>
20. Bulychev, S. I., Alehin, V. P. (1990). *Ispytanie materialov nepreryvnym vdvavlivaniem indentora*. Moscow: Mashinostroenie, 224.
21. Radko, I., Marhon, M. (2016). Features of research of grip strength composite materials contact with electrical worn parts. *Machinery and Energetics*, 252, 176–185. Available at: <http://journals.nubip.edu.ua/index.php/Tekhnica/article/view/8084/7735>
22. GOST 25.506–85. Design, calculation and strength testing. Methods of mechanical testing of metals. Determination of fracture toughness characteristics under the static loading. Moscow: Izdatel'stvo standartov, 62. Available at: <https://docs.cntd.ru/document/1200004652>
23. Podrezov, Yu. M., Verbylo, D. G., Danylenko, V. I., Tsyganenko, N. I., Shurygin, B. V., Romanko, P. M. (2018). Express method for prediction of long-term strength and creep resistance of high-temperature titanium-based alloys. *Elektronnaya mikroskopiya i prochnost' materialov*. Seriya: Fizicheskoe materialovedenie, struktura i svoystva materialov, 24, 35–46. Available at: <http://docplayer.net/171359405-Ekspres-metod-prognozuvannya-dovgotrivaloyi-micnosti-ta-oporu-povzuchosti-v-visokotemperaturnih-splavah-na-osnovi-titanu.html>
24. Fomin, O., Lovska, A., Pištěk, V., Kučera, P. (2019). Dynamic load effect on the transportation safety of tank containers as part of combined trains on railway ferries. *Vibroengineering PROCEDIA*, 29, 124–129. doi: <https://doi.org/10.21595/vp.2019.21138>
25. Lovska, A., Fomin, O., Kučera, P., Pištěk, V. (2020). Calculation of Loads on Carrying Structures of Articulated Circular-Tube Wagons Equipped with New Draft Gear Concepts. *Applied Sciences*, 10 (21), 7441. doi: <https://doi.org/10.3390/app10217441>
26. Karban', O. V., Hazanov, E. N., Hasanov, O. L., Salamatov, E. I., Goncharov, O. Yu. (2010). Nasledstvennost' i modifikaciya nanostrukturnoy keramiki ZrO<sub>2</sub> v processe izgotovleniya. *Perspektivnye materialy*, 6, 76–85.
27. Kul'kov, S. N., Korolev, P. V., Mel'nikov, A. G. (1995). Fazovye prevrascheniya v poroshke dioksida cirkoniya posle impul'snogo nagruzheniya. *Izvestiya vuzov. Fizika*, 38 (1), 51–55.
28. Gevorkyan, E. S., Nerubatskiy, V. P., Chyshkala, V. O., Morozova, O. M. (2020). Aluminum oxide nanopowders sintering at hot pressing using direct current. *Modern scientific researches*, 14, 12–18.
29. Gevorkyan, E., Rucki, M., Sałaciński, T., Siemiątkowski, Z., Nerubatskiy, V., Kucharczyk, W. et. al. (2021). Feasibility of Cobalt-Free Nanostructured WC Cutting Inserts for Machining of a TiC/Fe Composite. *Materials*, 14 (12), 3432. doi: <https://doi.org/10.3390/ma14123432>
30. Golovin, Yu. I. (2009). Nanoindentirovanie kak sredstvo kompleksnoy ocenki fiziko-mehaničeskikh svoystv materialov v submikroob'emah. *Zavodskaya laboratoriya. Diagnostika materialov*, 75 (1), 45–59.
31. Tret'yakov, Yu. D. (1978). *Tverdofaznye reakcii*. Moscow: Himiya, 360.
32. Raychenko, A. I. (1987). Vliyanie skorosti nagreva na poroobrazovanie v ul'tradisperstnykh poroshkah. *Metallurgiya*, 5, 14–18.
33. Panova, T. I., Arsent'ev, M. Yu., Morozova, L. V., Drozdova, I. A. (2010). Sintez i issledovanie nanokristallicheskoj keramiki v sisteme ZrO<sub>2</sub>-SeO<sub>2</sub>-Al<sub>2</sub>O<sub>3</sub>. *Fizika i himiya stekla*, 36 (4), 585–595.
34. Chyshkala, V. O., Lytovchenko, S. V., Gevorkyan, E. S., Nerubatskiy, V. P., Morozova, O. M. (2021). Structural phase processes in multicomponent metal ceramic oxide materials based on the system Y-Ti-Zr-O (Y<sub>2</sub>O<sub>3</sub>-TiO<sub>2</sub>-ZrO<sub>2</sub>). *SWorldJournal*, 7, 17–32. Available at: <https://www.sworldjournal.com/index.php/swj/article/view/swj07-01-008>
35. Latella, B. A., Henkel, L., Mehrtens, E. G. (2006). Permeability and high temperature strength of porous mullite-alumina ceramics for hot gas filtration. *Journal of Materials Science*, 41 (2), 423–430. doi: <https://doi.org/10.1007/s10853-005-2654-8>
36. Nettleship, I., Stevens, R. (1987). Tetragonal zirconia polycrystal (TZP) – A review. *International Journal of High Technology Ceramics*, 3 (1), 1–32. doi: [https://doi.org/10.1016/0267-3762\(87\)90060-9](https://doi.org/10.1016/0267-3762(87)90060-9)
37. Sakka, Y., Suzuki, T. S., Morita, K., Nakano, K., Hiraga, K. (2001). Colloidal processing and superplastic properties of zirconia- and alumina-based nanocomposites. *Scripta Materialia*, 44 (8-9), 2075–2078. doi: [https://doi.org/10.1016/s1359-6462\(01\)00889-2](https://doi.org/10.1016/s1359-6462(01)00889-2)
38. Gevorkyan, E. S., Nerubatskiy, V. P., Gutsalenko, Yu. H., Morozova, O. M. (2020). Some features of ceramic foam filters energy efficient technologies development. *Modern engineering and innovative technologies*, 14, 54–68. Available at: <http://repo.knmu.edu.ua/bitstream/123456789/28043/1/Article%2c%2011.2020.pdf>
39. Hevorkian, E. S., Nerubatskiy, V. P. (2009). Do pytan'nia otryman'nia tonkodispersnykh struktur z nanoporoshkiv oksydu aliuminiyu. *Zbirnyk naukovykh prats Ukrain'skoi derzhavnoi akademii zaliznychnoho transportu*, 111, 151–167. Available at: <http://lib.kart.edu.ua/handle/123456789/4418>
40. Hevorkian, E. S., Nerubatskiy, V. P. (2009). Modeliuvannia protsesu hariachoho presuvannia Al<sub>2</sub>O<sub>3</sub> pry priamomu propuskanni zminnoho elektrychnoho strumu z chastotoiu 50 Hts. *Zbirnyk naukovykh prats Ukrain'skoi derzhavnoi akademii zaliznychnoho transportu*, 110, 45–52. Available at: <http://lib.kart.edu.ua/handle/123456789/4416>
41. Marmer, N. E., Balaklienko, Yu. M., Novozhilov, S. A., Horasanov, O. L., Dvili, E. S. (2007). Vakuumnoe spekanie keramiki iz nanoporoshkov oksida cirkoniya. *Al'ternativnaya energetika i ekologiya*, 6 (50), 41–43. Available at: <https://cyberleninka.ru/article/n/vakuumnoe-spekanie-keramiki-iz-nanoporoshkov-okside-tsirkoniya>
42. Tokita, M. (2004). Mechanism of spark plasma sintering. *Journal of Materials Science*, 5 (45), 78–82.
43. Yoshimura, M., Ohji, T., Sando, M., Choa, Y.-H., Sekino, T., Niihara, K. (1999). Synthesis of nanograined ZrO<sub>2</sub>-based composites by chemical processing and pulse electric current sintering. *Materials Letters*, 38 (1), 18–21. doi: [https://doi.org/10.1016/s0167-577x\(98\)00125-6](https://doi.org/10.1016/s0167-577x(98)00125-6)

44. Fomin, O., Lovska, A. (2020). Establishing patterns in determining the dynamics and strength of a covered freight car, which exhausted its resource. *Eastern-European Journal of Enterprise Technologies*, 6 (7 (108)), 21–29. doi: <https://doi.org/10.15587/1729-4061.2020.217162>
45. Grabis, J., Steins, I., Rasmene, D., Krumina, A., Berzins, M. (2006). Preparation and characterization of  $ZrO_2-Al_2O_3$  particulate nanocomposites produced by plasma technique. *Proceedings of the Estonian academy of sciences, engineering*, 12 (4), 349–357. Available at: [https://www.kirj.ee/public/va\\_te/eng-2006-4-3.pdf](https://www.kirj.ee/public/va_te/eng-2006-4-3.pdf)
46. Gevorkyan, E. S., Nerubatskiy, V. P., Chyshkala, V. O., Morozova, O. M. (2021). Cutting composite material based on nanopowders of aluminum oxide and tungsten monocarbide. *Modern engineering and innovative technologies*, 15, 6–14. Available at: <http://repo.knmu.edu.ua/bitstream/123456789/28472/1/%D0%A1%D1%82%D0%B0%D1%82%D1%8C%D1%8F%2002.2021%20%D0%93%D0%B5%D1%80%D0%BC%D0%B0%D0%BD%D0%B8%D1%8F.pdf>
47. Samsonov, G. V. (Eds.) (1969). *Fiziko-himicheskie svoystva okislov*. Moscow: Metallurgiya, 455.
48. Buyakova, S. P., Horischenko, Yu. A., Kul'kov, S. N. (2004). Struktura, fazovyy sostav i morfologicheskoe stroenie plazmohimicheskikh poroshkov  $ZrO_2(MgO)$ . *Ogneupory i tehnikeskaya keramika*, 6, 25–30.
49. Davar, F., Hassankhani, A., Loghman-Estarki, M. R. (2013). Controllable synthesis of metastable tetragonal zirconia nanocrystals using citric acid assisted sol–gel method. *Ceramics International*, 39 (3), 2933–2941. doi: <https://doi.org/10.1016/j.ceramint.2012.09.067>
50. Gremillard, L., Chevalier, J., Epicier, T., Deville, S., Fantozzi, G. (2004). Modeling the aging kinetics of zirconia ceramics. *Journal of the European Ceramic Society*, 24 (13), 3483–3489. doi: <https://doi.org/10.1016/j.jeurceramsoc.2003.11.025>
51. Nikitin, D. S., Zhukov, V. A., Perkov, V. V. (2004). Poluchenie i struktura poristoy keramiki iz nanokristallicheskogo dioksida cirkoniya. *Neorganicheskie materialy*, 40 (7), 869–872.